MATHEMATICAL MODELING OF THE EFFECTS OF AEROBIC AND ANAEROBIC CHELATE BIODEGRADATION ON ACTINIDE SPECIATION

J. E. Banaszak, J. VanBriesen, and B. E. Rittmann
Northwestern University
Evanston. IL 60208-3109
USA

D. T. Reed
Argonne National Laboratory
Argonne, IL 60439
USA

Submittal for Proceedings to Migration '97

DISCLAIMER

DISCLAIMER

Portions of this document may be illegible in electronic image products. Images are produced from the best available original document.

MATHEMATICAL MODELING OF THE EFFECTS OF AEROBIC AND ANAEROBIC CHELATE BIODEGRADATION ON ACTINIDE SPECIATION

J. E. Banaszak, J. VanBriesen, and B. E. Rittmann, Northwestern University, Evanston, Illinois 60208-3109 U.S.A.

D. T. Reed, Argonne National Laboratory, Argonne, Illinois 60439 U.S.A.

Abstract

Biodegradation of natural and anthropogenic chelating agents directly and indirectly affects the speciation, and, hence, the mobility of actinides in subsurface environments. We combined mathematical modeling with laboratory experimentation to investigate the effects of aerobic and anaerobic chelate biodegradation on actinide [Np(IV/V), Pu(IV)] speciation. Under aerobic conditions, nitrilotriacetic acid (NTA) biodegradation rates were strongly influenced by the actinide concentration. Actinide-chelate complexation reduced the relative abundance of available growth substrate in solution and actinide species present or released during chelate degradation were toxic to the organisms. Aerobic bioutilization of the chelates as electron-donor substrates directly affected actinide speciation by releasing the radionuclides from complexed form into solution, where their fate was controlled by inorganic ligands in the system. Actinide speciation was also indirectly affected by pH changes caused by organic biodegradation. The two concurrent processes of organic biodegradation and actinide aqueous chemistry were accurately linked and described using CCBATCH, a computer model developed at Northwestern University to investigate the dynamics of coupled biological and chemical reactions in mixed waste subsurface environments. CCBATCH was then used to simulate the fate of Np during anaerobic citrate biodegradation. The modeling studies suggested that, under some conditions, chelate degradation can increase Np(IV) solubility due to carbonate complexation in closed aqueous systems.

Keywords: actinides, speciation, biological effects, coupled modeling, chelates, biodegradation

Introduction

Strong metal chelators are found in subsurface environments as a result of natural and anthropogenic processes. The presence of chelates in subsurface sites contaminated with actinides can increase the solubility of actinide species, causing accelerated migration [1-4]. Subsequent chelate biodegradation by subsurface organisms can result in the immobilization of actinide species due to precipitation reactions, sorption reactions, or the formation of complexes with other ligands in the system [5-7]. Therefore, the ultimate fate of actinides in subsurface aquifers containing chelators is related to the geochemistry and microbiology of the site.

Accurate modeling of actinide fate during chelate degradation requires systematic coupling of the interrelated effects of actinide chemical speciation and biological activity [8]. The presence of actinides can affect the activity of microorganisms in several ways. Specifically, at micro-molar concentrations, actinides can be toxic to microorganisms due to radiolytic effects and the chemical toxicity of aquo species [9, 10, 11]. Complexation, precipitation, and microbial resistance mechanisms can mitigate this

toxicity [8, 9, 11]. Additionally, formation of metal-chelate complexes lowers the concentration of chelate species that are substrates for bacteria, decreasing the rate at which organisms can degrade the organic compound [5, 6, 12-14].

In turn, biological processes can affect the chemical speciation of actinides. Microbiological degradation reactions routinely produce or consume hydrogen ions, causing changes in the pH of aqueous systems that can affect actinide solubility [8, 9, 15]. Additionally, biodegradation of organic compounds usually produces carbon dioxide. In a closed aqueous system, the resulting buildup of carbonate in solution can increase the concentration of soluble actinide species by forming actinide-carbonate complexes [16]. Alternatively, carbonate buildup can decrease actinide solubility by forming solid carbonate phases [16]. However, these effects can be mitigated by the activity of autotrophic microorganisms that utilize carbonate species as sources of cellular carbon for growth. Finally, biological depletion of common electron acceptors can alter the redox potential of the surrounding system, possibly shifting the oxidation state distribution of multi-valent actinides [17-19].

The purpose of this research is to use mathematical modeling to investigate the interrelated effects of chemical speciation and biological activity in model systems containing actinides and organic chelating agents. The computer program CCBATCH [15], developed at Northwestern University, is used to interpret experimental data determined in Pu(IV)- and Np(V)-NTA-*Chelatobacter heintzii* systems. The model results show that in the Np(V)-NTA system, the presence of Np affects NTA biodegradation due to toxicity of the aquo NpO_2^+ species towards *C. heintzii*, while Pu(IV) may inhibit NTA degradation due to a combination of toxicity and speciation effects. When the toxicity of the aquo NpO_2^+ species is mitigated by the presence of alternative complexing ligands, the pH increase caused by NTA degradation results in precipitation of the actinide from solution. Finally, modeling studies of anaerobic citrate degradation suggest that, under some conditions, chelate degradation can increase Np(IV) solubility due to carbonate complexation in closed aqueous systems.

Materials and Methods

Experimental

The detailed materials and methods used in this study were described previously [9, 10]. Briefly,
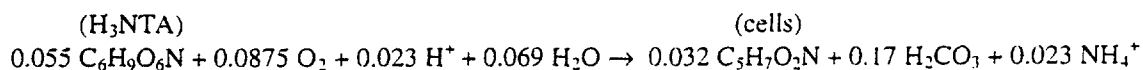
2

Chelatobacter heintzii (ATCC 29600), an obligately aerobic NTA degrader, was grown in a defined NTA culture medium [20] to log phase and used to inoculate sterile actinide-NTA samples in 40-ml serum bottles. Fixed-pH solutions were buffered with 0.01 M PIPES (piperazine-N, N'-bis[2-ethanesulfonic acid]). Variable-pH solutions were buffered with 12 mM phosphate. Actinide concentrations were measured by alpha scintillation counting (PACKARD Model 2500TR). Actinide speciation and oxidation state distribution were monitored by visible absorption spectroscopy (Varian CARY 5). The NTA analyses were performed with ion chromatography (Dionex DX-500).

Chemical Speciation Calculations

All chemical equilibrium calculations and modeling simulations were performed using CCBATCH. The exact modeling methodology is describe elsewhere [15]. To summarize, the model is unique in that it explicitly couples biological electron-donor and -acceptor substrate consumption to competing chemical reactions. In this way, CCBATCH determines the effects of biological reactions on the fate of various components in the system. The numerical solution method is similar to that implemented in several commonly used software packages for chemical speciation modeling in batch systems (e.g., MINTEQA2 [21], PHREEQE [22], and The Geochemist's Workbench [23]). All formation constants used (see Tables 1-4) were obtained for or corrected to the ionic strength of the growth medium (for NTA experiments) or to 0.1 M (for the citrate degradation simulations).

Biodegradation Calculations

To accurately predict the effects of chelate biodegradation on actinide speciation, the chemical effects of the biodegradation reactions must first be assessed. Using the method developed by McCarty [24], the aerobic biodegradation of NTA to mineralized products can be described by the following stoichiometry [15]:

$$\text{(H}_3\text{NTA)} \qquad\qquad\qquad \text{(cells)}$$
$$0.055\ C_6H_9O_6N + 0.0875\ O_2 + 0.023\ H^+ + 0.069\ H_2O \rightarrow 0.032\ C_5H_7O_2N + 0.17\ H_2CO_3 + 0.023\ NH_4^+$$

where $C_5H_7O_2N$ represents biomass.

Inspection of the reaction stoichiometry explains the pH rise observed in weakly buffered systems undergoing NTA degradation [9]. Because $HNTA^{2-}$ is the dominant NTA species at near-neutral pH, each mole of NTA mineralized consumes 2.42 acid equivalents: 2 equivalents due to loss of H_3NTA

3

and 0.023/0.055 = 0.42 equivalents to fulfill stoichiometric requirements. The magnitude of the pH rise depends on the concentration of buffers in the system, which may include a portion of the 3.4 moles of carbonic acid produced per mole of NTA degraded or intermediate degradation products [25]. In a closed aqueous system, retention of carbonic acid causes a less dramatic pH increase as compared to a solution in equilibrium with atmospheric $CO_2(g)$. In a natural subsurface system, biological production or consumption of hydrogen ions may not cause a large change in pH because of the buffering capacity of the surrounding minerals [26, 27].

The speciation part of CCBATCH calculates the pH effects of acid consumption or production caused by microbially catalyzed reactions. The number of hydrogen ions produced or consumed in biological respiration reactions is dependent on the combination of electron-donor and -acceptor substrates used. Table 1 shows the calculated stoichiometry for citrate biodegradation involving various electron acceptors. The results illustrate two key features of organic biodegradation reactions. First, the amount of biomass produced during citrate degradation is directly dependent on the electron-acceptor substrate; anaerobic biotransformation reactions produce much less biomass per mole of organic degraded, resulting in lower degradation rates. Second, the number of hydrogen ions produced or consumed per mole of electron-donor substrate degraded is related to the actual chemical form of the electron-donor substrate. Table 1 was constructed based on the assumption that H_3Cit is the biologically active substrate. If another citrate species is the actual substrate, the hydrogen ion column must be adjusted accordingly to reflect the change in the biodegradation reaction.

The rate of NTA or citrate biodegradation is mathematically represented by the Monod relationship [28], in which the rate-controlling electron-donor substrate concentration is the chelate species that is available to the bacteria. Metal chemical toxicity decreases the rate of biodegradation reactions and often exhibits saturation-type behavior. In these cases, metal toxicity can be described by adding the following term to adjust the maximum rate of substrate utilization [29]:

$$\frac{K_{Me}}{K_{Me} + [Me]}$$

As the concentration of the actual toxic metal species, [Me], becomes much greater than the constant K_{Me} (usually determined experimentally), microbial growth and substrate utilization slow and eventually are totally inhibited.

Results and Discussion

Effect of Np(V) on aerobic NTA biodegradation by *Chelatobacter heintzii*

The fate of actinides (An) during the biodegradation of organic chelating agents depends on the oxidation state of the metal [8]. In general, An(V) species show higher solubility and lower tendency toward complexation with most organic and inorganic ligands than do the An(III), An(IV), and An(VI) oxidation states [19, 30]. Previous research [9] on the aerobic Np(V)-NTA-*Chelatobacter heintzii* system showed that the aquo NpO_2^+ ion was toxic to the organism, but that the toxicity was mitigated by complexation with other inorganic ligands, allowing NTA degradation to proceed uninhibited at total Np concentrations up to 1.2×10^{-4} M. In this work, we use mathematical modeling to differentiate between growth inhibition due to actinide toxicity and decreased substrate utilization caused by chemical speciation effects.

In the case of organic chelate substrates, often only uncomplexed chelate species or specific metal-chelate complexes are the substrates for bacteria [5, 14, 31-33]. Thus, the microbial substrate utilization rate will remain unaffected by the presence of actinides (in the absence of toxic effects) as long as the concentration of the degradable substrate species remains high enough to support the growth of the degrading organisms. This is the case when the total amount of chelate in the system is much greater than the concentration of the actinide in solution, or when the actinide in near equal-molar solution has a relatively low formation constant with the chelate.

In the case of the Np-NTA system, equilibrium speciation calculations using the formation constants shown in Table 2 indicate that, in equal-molar Np-NTA solutions at pH 6.2, about 30% of the total NTA in solution remains uncomplexed. Because a significant fraction of uncomplexed NTA remains in this system, the modeling calculations shown in Figure 1 suggest that NTA biodegradation should remain unaffected by decreased substrate availability due to complexation at NTA:Np ratios of up to 1:1. However, the results of fixed-pH NTA degradation studies, also shown in Figure 1, clearly

indicate a lower than predicted rate of NTA degradation at an NTA:Np ratio of 10:1. Figure 1 illustrates that this reduced rate of NTA degradation is accurately described by accounting for the non-specific inhibitory (i.e., toxic) effect of the aquo NpO_2^+ ion on the degradation of NTA by *C. heintzii*.

In the Np-NTA system at fixed-pH, all the Np remained in solution following complete NTA degradation, primarily as the aquo species (data not shown). In contrast to the fixed-pH case, Banaszak et al. [9] showed that the pH increase caused by NTA degradation resulted in precipitation of the actinide from solution. Although these researchers were able to link the precipitate formed to the phosphoric acid system, they were not able to identify the solid phase. Subsequent to this work, Nash et al. [34] reported results describing the solubility of Np(V) in phosphate solutions as a function of Ca^{2+} concentration. Using these data, we were able to estimate an apparent solubility product of approximately 10^{-17}, based on the assumption that the solid formed was NpO_2CaPO_4.

Figure 2a shows the calculated equilibrium solubility of 1.2×10^{-4} M Np(V) in 12 mM phosphate solution during biodegradation of NTA. The model calculations suggest that two factors affect Np solubility. First, as NTA is degraded, re-equilibration of the system speciation increases the Np free ion concentration until it exceeds the solubility of the solid phase, initiating Np precipitation. Second, the increase in pH caused by NTA degradation increases the concentration of the PO_4^{3-} species by over one order of magnitude, which further increases the amount of Np precipitated from solution. The predicted removal of Np from solution is shown in Figure 2b, compared to the Np partitioning results reported by Banaszak et al. [9]. The agreement between model calculations and experimental measurements supports the hypothesis that Np is precipitated as a phosphate solid phase, possibly $NpO_2CaPO_4(s)$.

Effect of Pu(IV) on aerobic NTA biodegradation by *Chelatobacter heintzii*

In contrast to the An(V) oxidation state, the An(IV) oxidation state shows a higher propensity toward complexation with many organic and inorganic ligands [19, 30]. Thus, the formation of An(IV)-chelate complexes may retard the biological degradation of chelate substrates by decreasing the concentration of degradable substrate species. Reed and co-workers [10] showed that, in the Pu(IV)-NTA-*C. heintzii* system, NTA degradation was significantly slowed by increasing Pu concentrations, but they were not able to determine if the reduction in NTA degradation rate was due solely to the

6

radiotoxicity of bioassociated Pu or if there was a contribution from speciation effects.
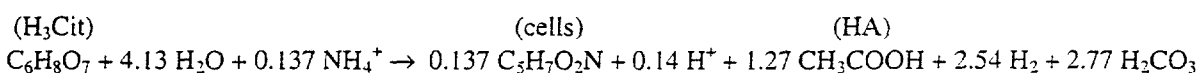
Figure 3a shows the model-calculated degradation of NTA, in the presence of varying Pu concentrations, compared to experimental results reported by Reed et al. [10]. Because there remains considerable controversy over the aqueous speciation of Pu(IV) at near-neutral pH, model calculations were performed for two sets of Pu(IV)-hydroxide and -carbonate formation constants, listed in Table 3. Figure 3a shows that calculations based on stepwise formation constants for Pu(IV)-hydroxide and -carbonate complexes closely match those based on the formation of mixed hydroxide-carbonate complexes. Also, experimental evidence that NTA dissolves the Pu(IV) polymer [10, 35] suggests that the reported formation constants for the $PuNTA^+$ complex [36] may be several orders of magnitude too low; so a formation constant of log K=25 was used for all modeling simulations to investigate if an exceptionally stable complex could reduce the degradable substrate concentration enough to explain the retarded NTA degradation observed. Even in this extreme case, the modeling results shown in Fig. 3a cannot account for the observed residual NTA in solution. In each case, the residual ligand-to-metal ratio is greater than 1:1. By assuming that Pu-NTA complexes with ligand-to-metal ratios greater than 1:1 dominate Pu speciation, we are able to predict the long-term residual Pu:NTA ratio, as is shown in Figure 3b. However, the model calculations still do not account for the slower NTA degradation noted in the Pu-containing samples at times less than 10 hours, supporting the conclusion that radiotoxicity contributed to the lower rate of NTA degradation [10]. Although this modeling work suggests that chemical speciation effects may contribute to slower NTA degradation, more research is needed to confirm that complexation reduces substrate availability in this system.

Predicted fate of Np(IV) during the degradation of citric acid by an anaerobic microbial consortium

Under anaerobic conditions, the complete degradation of organic compounds is often catalyzed by a consortium of microorganisms. In many subsurface systems, mineralization of organic compounds increases the total aqueous carbonate concentration because of decreased carbonate exchange with the gas phase. However, increasing carbonate concentrations can be attenuated by autotrophic microorganisms that use inorganic carbon as carbon sources for growth. To investigate the fate of Np(IV) during the degradation of the organic chelate citric acid, we used coupled modeling to calculate

the equilibrium concentration of soluble Np(IV/V) species in a closed aqueous system under the following initial conditions: pH 6; total carbonate concentration of 10^{-5} M; a fixed redox potential of -250 mV, a level at which organic compound fermentation and biological methane production are possible [27]; and equilibrium with the $Np(OH)_4(am)$ solid phase [37]. The formation constants used for this work are shown in Table 4.

We assumed that, in this model system, the degradation of citric acid was catalyzed by an anaerobic microbial consortium consisting of three organisms: citrate-fermenting bacteria, acetate-cleaving methanogens, and hydrogen-oxidizing methanogens. In the first step, citric acid (H_3Cit) is fermented to acetic acid (HA) and hydrogen. The stoichiometry of this reaction is found in Table 1:

(H$_3$Cit)   (cells)   (HA)
$$C_6H_8O_7 + 4.13\ H_2O + 0.137\ NH_4^+ \rightarrow 0.137\ C_5H_7O_2N + 0.14\ H^+ + 1.27\ CH_3COOH + 2.54\ H_2 + 2.77\ H_2CO_3$$

Two organisms consume the products of this reaction. Acetoclastic methanogens form methane and carbonic acid from acetic acid:

(HA)   (cells)
$$CH_3COOH + 0.901\ H_2O + 0.0181\ NH_4^+ \rightarrow 0.0181\ C_5H_7O_2N + 0.018\ H^+ + 0.955\ CH_4 + 0.955\ H_2CO_3$$

and hydrogen-oxidizing methanogens produce methane by coupling the oxidation of H_2 to the reduction of carbonic acid, while fixing inorganic carbon as a source of cellular carbon for biosynthesis:

(cells)
$$4\ H_2 + 1.04\ H_2CO_3 + 0.017\ NH_4^+ \rightarrow 0.017\ C_5H_7O_2N + 0.958\ CH_4 + 3.09\ H_2O + 0.017\ H^+$$
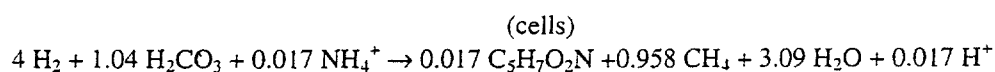
All three reactions affect the carbonate concentration and pH of the system.

Figure 4 shows the results of model calculations under the stated conditions and illustrates several key points regarding the complexity of this relatively simple model system. The initial degradation of citrate, a relatively strong actinide chelator, results in an increase in pH and a slight decrease in Np solubility. However, because carbonate is retained in a closed system, the carbonate produced by the citrate and acetate degradation reactions, coupled with the pH increase due to the same two reactions, results in a 2-3 order of magnitude *increase* in soluble Np species. Although these effects are mitigated somewhat by the activity of hydrogen-oxidizing methanogens, the total Np solubility remains elevated following consumption of all the available hydrogen (not shown). Thus, although we might predict *a priori* that degradation of organic chelates in reducing environments decreases actinide

8

mobility, careful linking of chemical and microbiological effects suggests that, in some cases, the opposite may be true. In the example just given, coupled modeling shows us that anaerobic degradation of citrate leads to the buildup of carbonate and a net increase in Np solubility.

Conclusions

Mathematical modeling was used to couple biological and chemical reactions to predict the fate of actinides in several model systems. In the Np(V) system, degradation of NTA in the absence of other ligands resulted in the inhibition of microbial activity due to the toxicity of the aquo Np(V) species. In the presence of phosphate, however, NTA degradation proceeded uninhibited and resulted in the precipitation of the actinide from solution. In contrast, NTA degradation in the Pu(IV) system was significantly slowed by the presence of the actinide in complexed form. Reduced substrate availability due to Pu(IV)-NTA complexation may have contributed to the observed decrease in NTA degradation. Finally, coupled modeling was used to predict conditions under which Np(IV) solubility can be increased during chelate biodegradation.

Acknowledgments

References

1. Baik, M. H. and K. J. Lee, *Annals of Nuclear Energy* **21**, 81 (1994).
2. Riley, R. G., J. M. Zachara, and F. J. Wobber. (1992). "Chemical Contaminants on DOE lands and Selection of Contaminant Mixtures for Subsurface Science Research." *DOE/ER-0547T*, Office of Energy Research, U.S. Department of Energy, Washington, DC.
3. Reed, D. T., J. M. Zachara, R. E. Wildung, and F. J. Wobber, *in* "Materials Research Society Symposium Proceedings", Vol. 212, p. 765, 1991.
4. Means, J. L., D. A. Crerar, and J. O. Duguid, *Science* **200**, 1477 (1978).
5. Bolton, H. J., D. Girvin, A. Plymale, S. Harvey, and D. Workman, *Environmental Science and Technology* **30**, 931 (1996).
6. Francis, A., C. Dodge, and J. Gillow, *Nature* **356**, 140 (1992).
7. Dozol, M. and R. Hagemann, *Pure and Applied Chemistry* **65**, 1081 (1993).
8. Banaszak, J. E., D. T. Reed, and B. E. Rittmann, *Journal of Radioanalytical and Nuclear Chemistry* (accepted).
9. Banaszak, J. E., D. T. Reed, and B. E. Rittmann, *Environmental Science and Technology* (accepted).
10. Reed, D. T., Y. Vojta, J. W. Quinn, and M. K. Richmann, *Radiochimica Acta* (submitted).
11. Plummer, E. J. and L. E. Macaskie, *Bulletin of Environmental Contamination and Toxicology* **44**, 143 (1990).
12. Brynhildsen, L. and B. Allard, *Biometals* **7**, 163 (1994).

13.   Francis, A. and C. Dodge, *Applied and Environmental Microbiology* **59**, 109 (1993).

14.   Joshi-Topé, G. and A. Francis, *Journal of Bacteriology* **177**, 1989 (1995).

15.   Rittmann, B. E. and J. M. VanBriesen, *in* "Reviews in Mineralogy" (P. C. Lichtner, C. I. Steefel, and E. H. Oelkers., eds.), Vol. 34: Reactive Transport in Porous Media, p. 311. Mineralogical Society of America, 1996.

16.   Clark, D. L., D. E. Hobart, and M. P. Neu, *Chemical Reviews* **95**, 25 (1995).

17.   Choppin, G. R. and A. H. Bond, *Journal of Analytical Chemistry* **51**, 1129 (1996).

18.   Hakanen, M. and A. Lindberg. (1995). "Technetium, Neptunium and Uranium in Simulated Anaerobic Groundwater Conditions." *YJT-95-02*, Voimayhtiöiden Ydinjätetoimikunta (Nuclear Waste Commission of Finnish Power Companies), Helsinki.

19.   Silva, R. J. and H. Nitsche, *Radiochimica Acta* **70/71**, 377 (1995).

20.   Tiedje, J. M., B. B. Mason, C. B. Warren, and E. J. Malec, *Applied Microbiology* **25**, 811 (1973).

21.   Allison, J. D., D. S. Brown, and K. J. Nono-Gradac. (1991). "MINTEQA2/PRODEFA2, A Geochemical Assessment Model for Environmental Systems: Version 3.0 User's Manual." *EPA/600/3-91/021*, U.S. Environmental Protection Agency, Athens, GA.

22.   Parkhurst, D. L., D. C. Thorstenson, and L. N. Plummer. (1980). "PHREEQE-A Computer Program for Geochemical Calculations." *PB81-167801*, National Technical Information Services Report, Springfield, VA.

23.   Bethke, C. M. (1992). "The Geochemist's Workbench, A User's Guide to Rxn, Act2, Tact, React, and Gtp[lot]." , Hydrogeology Program, University of Illinois, Champaign-Urbana, IL.

24.   McCarty, P. L., *in* "Proceedings: The International Conference Toward a Unified Concept of Biological Waste Treatment Design", p. 24, Atlanta, GA, 1972.

25.   VanBriesen, J. and B. E. Rittmann, (in preparation).

26.   Morel, F. M. M. and J. G. Hering, "Principles and Applications of Aquatic Chemistry," p. 588. John Wiley & Sons, New York, 1993.

27.   Stumm, W. and J. J. Morgan, "Aquatic Chemistry," p. 1022. John Wiley & Sons, Inc., New York, 1996.

28.   Monod, J., *Annual Reviews of Microbiology* **3**, 371 (1949).

29.   Rittmann, B. E. and P. B. Sáez, *in* "Biotreatment of Industrial and Hazardous Wastes" (M. Levin and M. Gealt, eds.), p. 113. McGraw-Hill Book Co, New York, 1993.

30.   Lieser, K. H., *Radiochimica Acta* **70/71**, 355 (1995).

31.   Bergsma, J. and W. N. Konings, *European Journal of Biochemistry* **134**, 151 (1983).

32.   Brynhildsen, L. and T. Rosswall, *Applied and Environmental Microbiology* **55**, 1375 (1989).

33.   Cachon, R. and S. D. Daniel, *FEMS Microbiology Letters* **131**, 319 (1995).

34.   Nash, K. L., L. R. Morss, M. P. Jensen, and M. Schmidt. (1996). "Phosphate Mineralization of Actinides by Measured Addition of Precipitating Anions." *CH2-6-C3-22*, Chemistry Division, Argonne National Laboratory, Argonne, IL.

35.   Al Mahamid, I., K. A. Becraft, N. L. Hakem, R. C. Gatti, and H. Nitsche, *Radiochimica Acta* **74**, 129 (1996).

36.   Nitsche, H. and K. Becraft, *in* "Tranuranium Elements - A Half Century" (L. R. Morss and J. Fuger, eds.), p. 276. American Chemical Society, Washington, DC, 1992.

37.   Pratopo, R. M., H. Moriyama, and K. Higashi, *in* "Proceedings of the 1989 Joint International Waste Management Conference", Vol. 2, p. 309, 1989.

38.   Neck, V., J. I. Kim, and B. Kanellakopulos, *Radiochimica Acta* **56**, 25 (1992).

39.   Lierse, C., W. Treiber, and J. I. Kim, *Radiochimica Acta* **38**, 27 (1985).

40.   Bidoglio, G., G. Tanet, and A. Chatt, *Radiochimica Acta* **38**, 21 (1985).

41.   Neck, V., W. Runde, J. I. Kim, and B. Kanellakopulos, *Radiochimica Acta* **65**, 29 (1994).

42.   Eberle, S. H. and U. Wede, *Journal of Inorganic Nuclear Chemistry* **32**, 109 (1970).

43.   Morgenstern, A. and J. I. Kim, *Radiochimica Acta* **72**, 73 (1996).

44.   Kim, J. I., C. Lierse, and F. Baumgartner, *in* "Plutonium Chemistry" (W. T. Carnall and G. R. Choppin, eds.), p. 319. American Chemical Society, Washington, DC, 1983.

45.   Nitsche, H., *in* "Materials Research Society Symposium Proceedings", Vol. 212, p. 517, 1991.

46.   Yamaguchi, T., Y. Sakamoto, and T. Ohnuki, *Radiochimica Acta* **66/67**, 9 (1994).

47.   Martell, A. E. and R. M. Smith, (eds.), "Critical Stability Constants." Plenum Press, New York, 1974-1989.

48.   Jones, A. D. and G. R. Choppin, *Actinides Reviews* **1**, 311 (1969).

49.   Pratopo, M. I., H. Moriyama, and K. Higashi, *Radiochimica Acta* **51**, 27 (1990).

Table 1. Citrate degradation stoichiometry using a variety of electron acceptors, as determined from energetic calculations developed by McCarty [24]. H_3Cit is chosen as the reference level for citric acid.

Energy Generation Mechanism	Electron Acceptor Couple (ox/red)	Biomass Yield (mole cells/mole citrate)	Electron Acceptor (mole consumed/mole citrate)	Acid Equivalents Produced (+) or Consumed (-)/ mole citrate	Carbonic Acid (mole produced/mole citrate)	NH_4^+ (mole consumed/ mole citrate)
Aerobic Citrate Respiration	H_2O/O_2	0.64	1.29	+0.64	2.79	0.64
Nitrate Reduction	$NO_3^-/N_2(g)$	0.63	1.07	-0.44	2.84	0.63
Manganese Reduction	$MnO_2(s)/Mn^{2+}$	0.60	2.97	-5.34	2.99	0.60
Iron Reduction	$Fe(OH)_3(s)/Fe^{2+}$	0.44	9.13	-17.8	3.78	0.44
Sulfate Reduction	SO_4^{2-}/H_2S	0.26	1.60	-2.95	4.70	0.26
Fermentation to $H_2(g)$ and Acetate	Citrate/Acetate and H_2	0.14	1.27 mole acetate produced/mole citrate	+1.41	2.77	0.14

Table 2. Complex formation constants for major neptunium(V) aqueous species in NTA mineral growth medium in equilibrium with atmospheric carbon dioxide

Species	$\beta_{xyz}{}^{a}$	References
NpO_2OH	$\beta_{1(-1)0} = 10^{-11.3}$	[38, 39]
$NpO_2(OH)_2{}^-$	$\beta_{1(-2)0} = 10^{-23.43}$	[38, 39]
$NpO_2CO_3{}^-$	$\beta_{101} = 10^{4.38}$	[16, 40, 41]
$NpO_2(CO_3)_2{}^{3-}$	$\beta_{102} = 10^{6.55}$	[16, 40, 41]
$NpO_2(CO_3)_3{}^{5-}$	$\beta_{103} = 10^{6.4}$	[16, 40, 41]
NpO_2NTA^{2-}	$\beta_{101} = 10^{6.80}$	[36, 42]
NpO_2HNTA^-	$\beta_{111} = 10^{1.77}$	[42]
$NpO_2(OH)NTA^{2-}$	$\beta_{1(-1)1} = 10^{-4.66}$	[42]
$NpO_2HPO_4{}^-$	$\beta_{111} = 10^{14.23}$	[43]
$NpO_2PO_4{}^{2-}$	$\beta_{101} = 10^{6.33}$	[43]

^{a} Where $\beta_{xyz} = \dfrac{[M_x H_y L_z]}{[M]^x[H]^y[L]^z}$ or $\beta_{x(-y)z} = \dfrac{[M_x(OH)_y L_z][H]^y}{[M]^x[L]^z}$.

Table 3. Complex formation constants for major plutonium(IV) aqueous species in NTA mineral growth medium in equilibrium with atmospheric carbon dioxide

Species	$\beta_{xyz}{}^a$	References
$PuOH^{3+}$	$\beta_{1(-1)0} = 10^{-1.80}$	[44]
$Pu(OH)_2{}^{2+}$	$\beta_{1(-2)0} = 10^{-3.40}$	[44]
$Pu(OH)_3{}^{+}$	$\beta_{1(-3)0} = 10^{-7.30}$	[44]
$Pu(OH)_4{}^{0}$	$\beta_{1(-4)0} = 10^{-11.70}$	[44]
$Pu(OH)_5{}^{-}$	$\beta_{1(-5)0} = 10^{-17.30}$	[44]
$PuCO_3{}^{2+}$	$\beta_{1(-2)1} = 10^{-3.71}$	[45]
$Pu(CO_3)_2{}^{0}$	$\beta_{1(-4)2} = 10^{-8.67}$	[45]
$Pu(CO_3)_3{}^{2-}$	$\beta_{1(-6)3} = 10^{-18.30}$	[45]
$Pu(CO_3)_4{}^{4-}$	$\beta_{1(-8)4} = 10^{-31.04}$	[45]
$Pu(CO_3)_5{}^{6-}$	$\beta_{1(-10)5} = 10^{-46.05}$	[45]
$Pu(OH)_2(CO_3)_2{}^{2-}$	$\beta_{1(-6)2} = 10^{-15.82}$	[46]
$Pu(OH)_4(CO_3)_2{}^{4-}$	$\beta_{1(-8)2} = 10^{-38.30}$	[46]

^{a} Where $\beta_{xyz} = \dfrac{[M_xH_yL_z]}{[M]^x[H]^y[L]^z}$ or $\beta_{x(-y)z} = \dfrac{[M_x(OH)_yL_z][H]^y}{[M]^x[L]^z}$.

Table 4. Complex formation constants for major neptunium(IV/V) aqueous species in citrate-containing systems in equilibrium with atmospheric carbon dioxide

Species	$\beta_{xyz}{}^a$	References
NpO_2Cit^{2-}	$\beta_{1(0)1} = 10^{3.67}$	[47]
NpO_2HCit^-	$\beta_{1(1)1} = 10^{2.69}$	[47]
$NpCit^+$	$\beta_{1(0)1} = 10^{15.84}$	From $PuCit^+$ [48]
$NpOH^{3-}$	$\beta_{1(-1)0} = 10^{-2.10}$	[16]
$Np(OH)_2{}^{2-}$	$\beta_{1(-2)0} = 10^{-5.32}$	estimate
$Np(OH)_3{}^-$	$\beta_{1(-3)0} = 10^{-8.55}$	estimate
$Np(OH)_4{}^0$	$\beta_{1(-4)0} = 10^{-11.80}$	[37, 46]
$Np(OH)_5{}^-$	$\beta_{1(-5)0} = 10^{-23.70}$	[16]
$NpCO_3{}^{2+}$	$\beta_{1(0)1} = 10^{12.30}$	[45]
$Np(CO_3)_2{}^0$	$\beta_{1(0)2} = 10^{23.35}$	[45]
$Np(CO_3)_3{}^{2-}$	$\beta_{1(0)3} = 10^{30.00}$	[45]
$Np(CO_3)_4{}^{4-}$	$\beta_{1(0)4} = 10^{33.00}$	[45]
$Np(CO_3)_5{}^{6-}$	$\beta_{1(0)5} = 10^{34.00}$	[45]
$Np(OH)_2(CO_3)_2{}^{2-}$	$\beta_{1(-2)2} = 10^{15.50}$	[46, 49]
$Np(OH)_4(CO_3)_2{}^{4-}$	$\beta_{1(-4)2} = 10^{-4.70}$	[46, 49]

^{a} Where $\beta_{xyz} = \dfrac{[M_xH_yL_z]}{[M]^x[H]^y[L]^z}$ or $\beta_{x(-y)z} = \dfrac{[M_x(OH)_yL_z][H]^y}{[M]^x[L]^z}$.
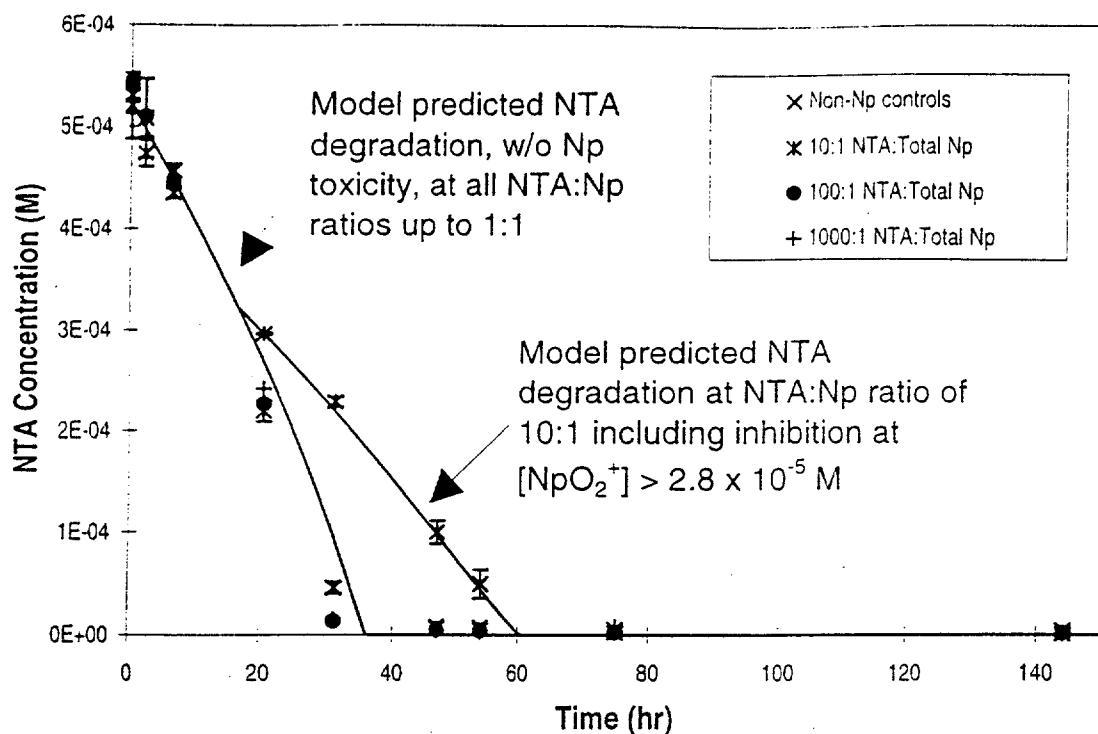
Fig. 1. Comparison cf actual to model-calculated NTA degradation by *Chelatobacter heintzii* in fixed-pH 6.1 minimal NTA growth medium, in equilibrium with atmospheric carbon dioxide, and in the presence of increasing total neptunium concentrations. Model calculations indicate that the inhibition of NTA degradation noted at an NTA:Np ratio of 10:1 can be correlated to chemical inhibition caused by the aquo NpO_2^+ species. Error bars are the 95% confidence limits for three non-rad controls and two 10:1 NTA:Np samples.
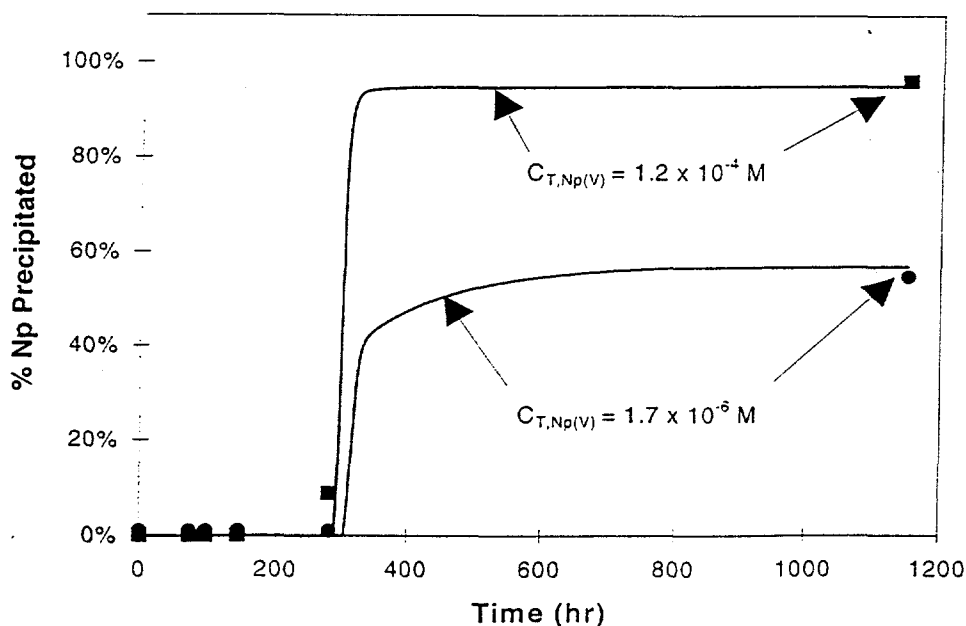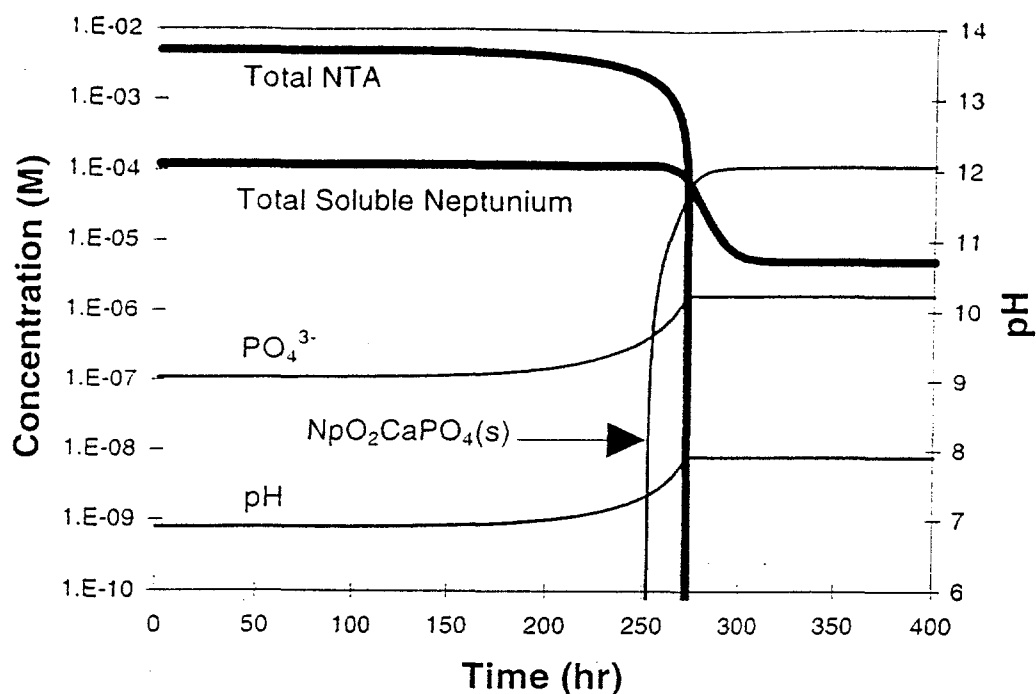
Fig. 2a (top). Calculated equilibrium speciation of 1.2×10^{-4} M Np during the degradation of NTA by *Chelatobacter heintzii*. The solution contains a 5 mM NTA mineral growth medium and 12 mM phosphate buffer and is in equilibrium with atmospheric carbon dioxide. Calculated results are based on precipitation of the assumed solid phase NpO_2CaPO_4. **Fig. 2b (bottom).** Comparison of model-calculated Np solubility to measured total Np concentrations after biodegradation of NTA. Neptunium precipitation was initiated by the biodegradation of NTA. Total Np solubility was further decreased by the pH increase associated with NTA degradation.
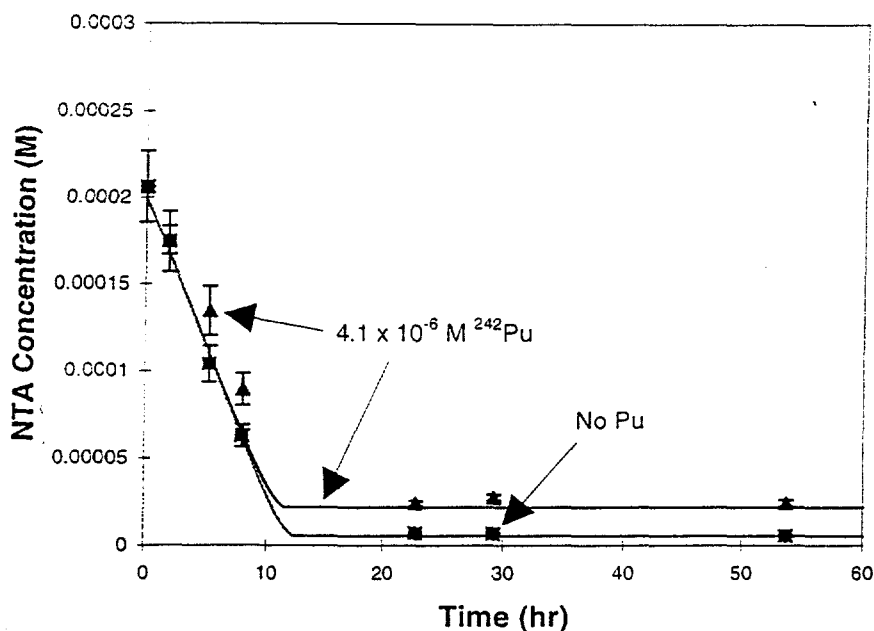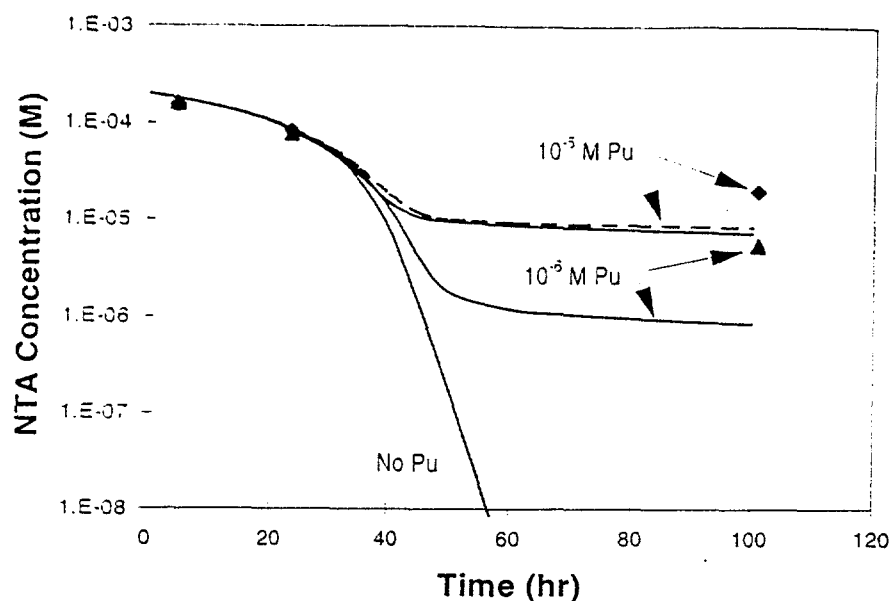
Fig. 3a (top). Model-calculated NTA degradation by *Chelatobacter heintzii* compared to experimental degradation results in fixed-pH 6.2 solutions that are in equilibrium with atmospheric carbon dioxide and contain 0, 10^{-6}, or 10^{-5} M ^{239}Pu. Experimental data points are the average of two samples. The two 10^{-5} M Pu simulations compare model calculations based on the hydroxide and carbonate equilibrium formation constants reported by Nitsche and Kim et al. (solid line) to calculations based on the constants reported by Yamaguchi et al. (dashed line). In every case, the model calculations overpredict the amount of NTA degraded after 100 hours. **Fig. 3b (bottom).** Comparison of model-calculated to experimental NTA degradation in the presence of 0 and 4.1 x 10^{-6} M ^{242}Pu when Pu(IV)-NTA complexes with ligand-to-metal ratios greater than 1:1 are considered. Even though the correct residual NTA concentration is predicted, model calculations do not accurately reflect the observed inhibition of NTA degradation at less than 10 hours. Error bars are 95% confidence limits.
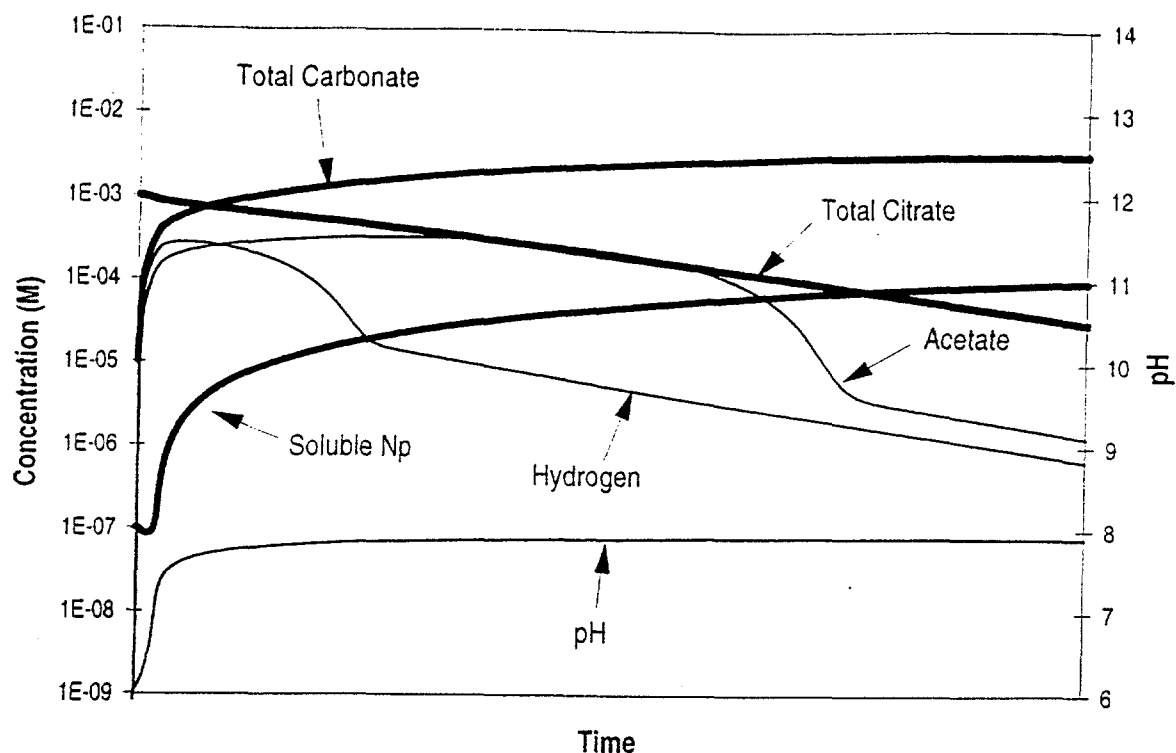
Fig. 4. Simulated fate of Np during the mineralization of citrate by an anaerobic microbial consortium consisting of citrate-fermenting bacteria, acetate-cleaving methanogens, and hydrogen-oxidizing methanogens. Methane production is omitted from the diagram for clarity. System is assumed closed to exchange with atmospheric carbon dioxide, at a fixed redox potential of -250 mV, and in equilibrium with Np(IV) hydrous oxide solid. Citrate fermentation and acetate cleavage to methane result in the production of carbonate species and an increase in system pH, causing Np solubility to increase during chelate degradation.